
VEC2FACE: SCALING FACE DATASET GENERATION WITH LOOSELY CONSTRAINED VECTORS

Anonymous authors

Paper under double-blind review

A APPENDIX

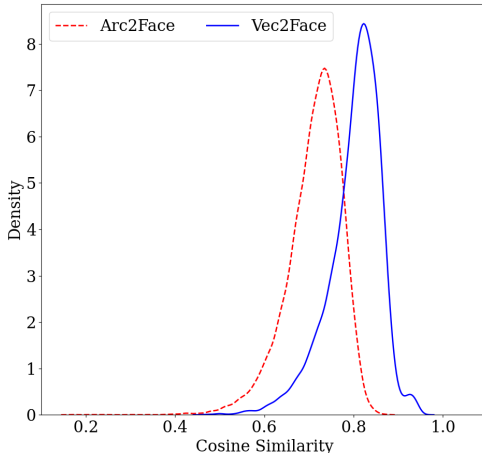


Figure 1: Similarity measurement between original and reconstructed in-the-wild images (LFW (Huang et al., 2008)).

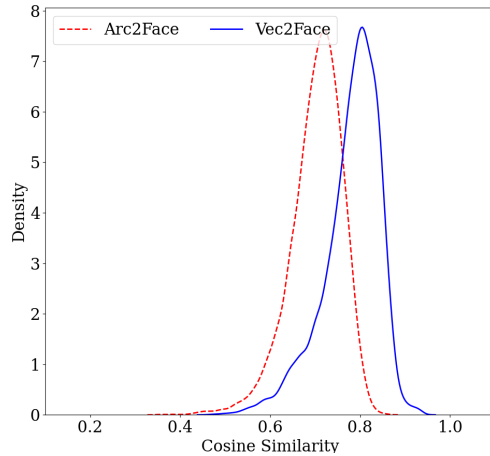


Figure 2: Similarity measurement between original and reconstructed Hadrian images (Wu et al., 2024).

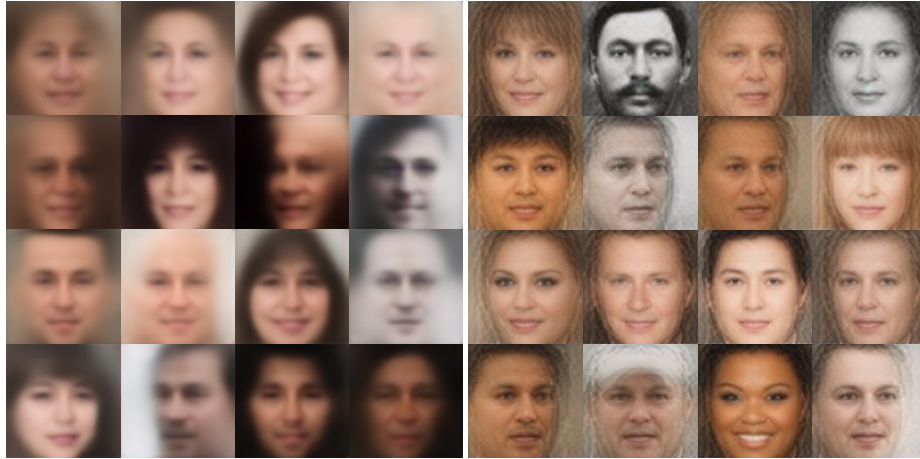
A.1 COMPARISON WITH DIFFUSION MODEL

Training a diffusion model conditioned with image feature vectors is a similar approach to Vec2Face. Thus, we evaluate both architectures by measuring the performance on open-set image reconstruction. For model choice, Arc2Face (Papantoniou et al., 2024) model, which fine-tunes the stable-diffusion-v1-5 on WebFace42M, is used to represent the diffusion models. For test set choices, the images in an in-the-wild dataset, LFW (Huang et al., 2008), and an indoor dataset, Hadrian (Wu et al., 2024) are used. Since both model use face feature as input, we extract image features by using a FR model and feed to both models for image reconstruction. **Because both dataset are trained/fine-tuned on the cropped and aligned FR datasets, no image cropping and alignment are used in this evaluation.** Fig. 1 and Fig. 2 show the similarity distribution between the original images and reconstructed images. The observations are: 1) both models can preserve the identity for the in-door images, 2) Vec2Face has better performance on open-set image reconstruction on both datasets, 3) the diffusion model conditioned with image/identity features do not always preserve the identity, especially for in-the-wild images. Since both model use the features of the same set of images and the variation of the images generated by Arc2Face are only dependent on the initial noise image, we speculate the failed cases of identity preservation are caused by the initial noise image. Hence, the proposed architecture is better than the conventional diffusion model conditioned with image features on identity preservation. Examples are shown in Fig. 11.

A.2 ABLATION STUDY OF LOSS FUNCTIONS

This section presents the effects of identity loss L_{id} , perceptual loss, L_{lips} and GAN loss L_{GAN} on image reconstruction. The observations in Fig. 3 are: 1) without perceptual loss, the reconstructed

054
055
056
057
058
059
060
061
062
063
064
065
066
067
068



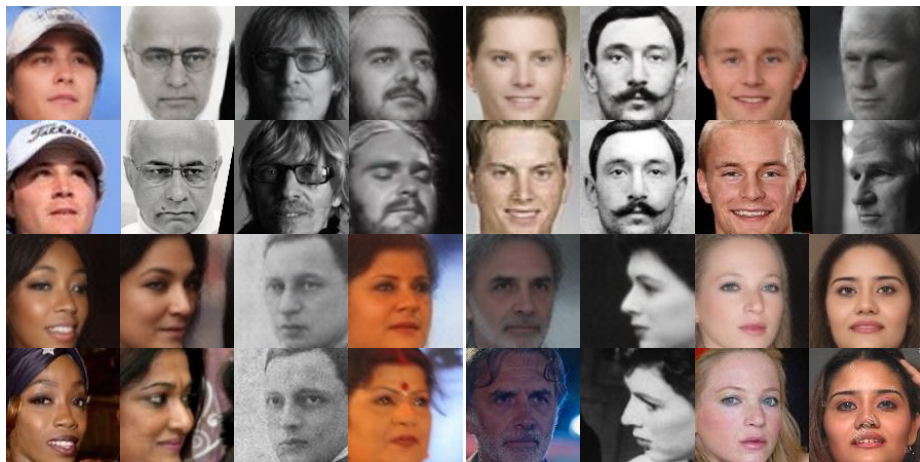
Effect of perceptual loss at epoch 138

069
070
071
072
073
074
075
076
077
078
079
080
081
082
083
084



Effect of GAN loss at epoch 34

085
086
087
088
089
090
091
092
093
094
095
096
097
098
099



Effect of identity loss

101
102
103
104
105
106
107

Figure 3: Examples of loss effect during training. The reconstructed examples with corresponding loss involved are on the left, otherwise on the right. For identity loss, odd rows are reconstructed images and even rows are original images.

face edges are smoothed, 2) involving GAN loss at an early training stage causes a glitch effect on image reconstruction, 3) without identity loss, Vec2Face performs well on near-frontal images but not on images with large pose variations.

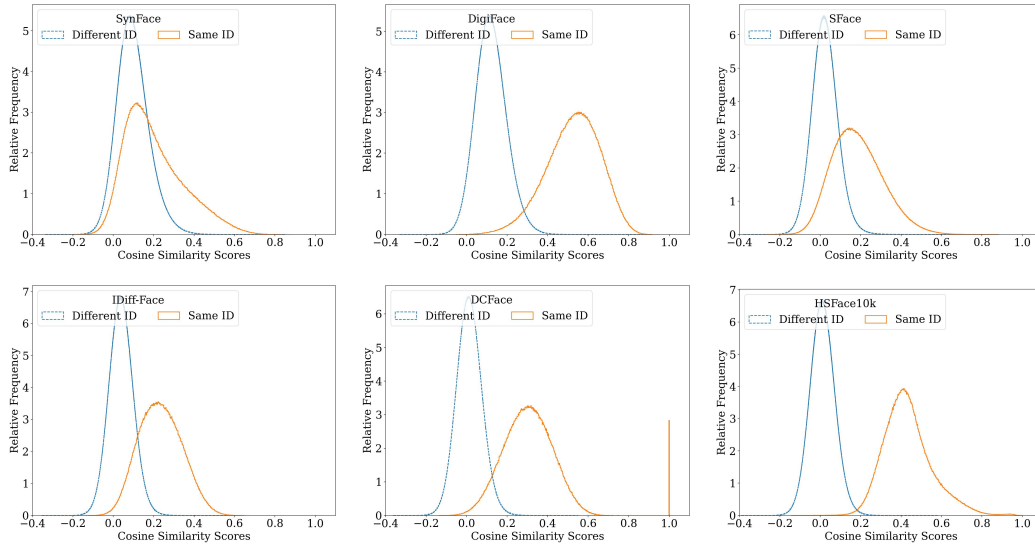


Figure 4: Similarity distributions of available synthetic datasets (Qiu et al., 2021; Boutros et al., 2022; Bae et al., 2023; Boutros et al., 2023; Kim et al., 2023) and ours. The results indicate that our dataset has the largest separability and smallest overlap / Equal Error Rate between genuine (**same ID**) and impostor (**different ID**) pairs.

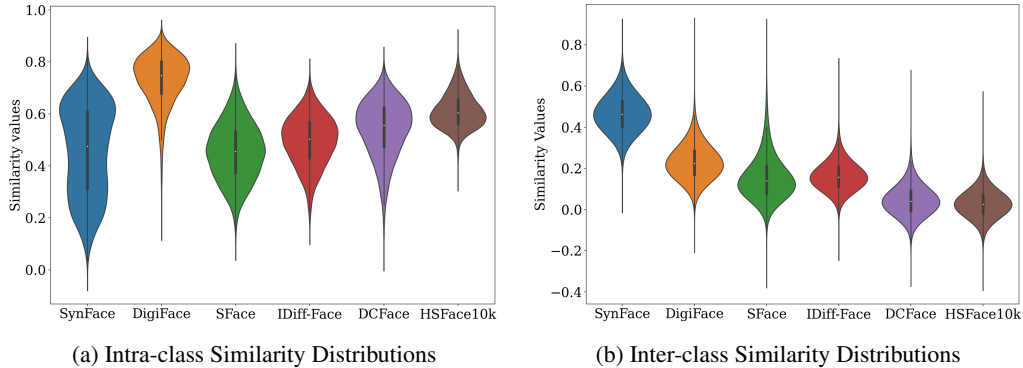


Figure 5: The inter-class and intra-class similarity distributions of the available synthetic datasets (Qiu et al., 2021; Boutros et al., 2023; Bae et al., 2023; Kim et al., 2023; Boutros et al., 2022) and ours.

A.3 SYNTHETIC FR DATASET NOISE ANALYSIS

Dataset noise could be categorized as: i) images from different identities are in the same identity folder, and ii) images from the same identity are in different identity folders. For synthetic datasets, there is no ground truth for identities, so we used the labels provided by the corresponding work.

Following the metric used in previous works (Cao et al., 2018; Wu & Bowyer, 2023; Zhu et al., 2023; Deng et al., 2022), we evaluate the dataset noise using two hard threshold values: one for detecting the outliers within each folder (intra-class noise), and another for detecting similar identities but marked as different in the dataset (inter-class noise). Figure 5a shows the cosine similarity distributions of the available synthetic datasets in situation one. Since greater similarity means images are more likely from the same identity, the results show that our dataset has the highest identity consistency within each identity folder. Moreover, if the similarity value of an image feature and its identity feature is less than 0.3, it can be regarded as an outlier/noise (Deng et al., 2022). With this metric, the available synthetic datasets contain greater intra-class noise than ours. Figure 5b shows the similarity distributions of available synthetic datasets in situation two. WebFace260M (Zhu et al., 2023) is the only work discussing the details of inter-class denoising. It merged two identity folders if their identities have higher than 0.7 similarity, so if the identity similarity is larger than 0.7, we regard it

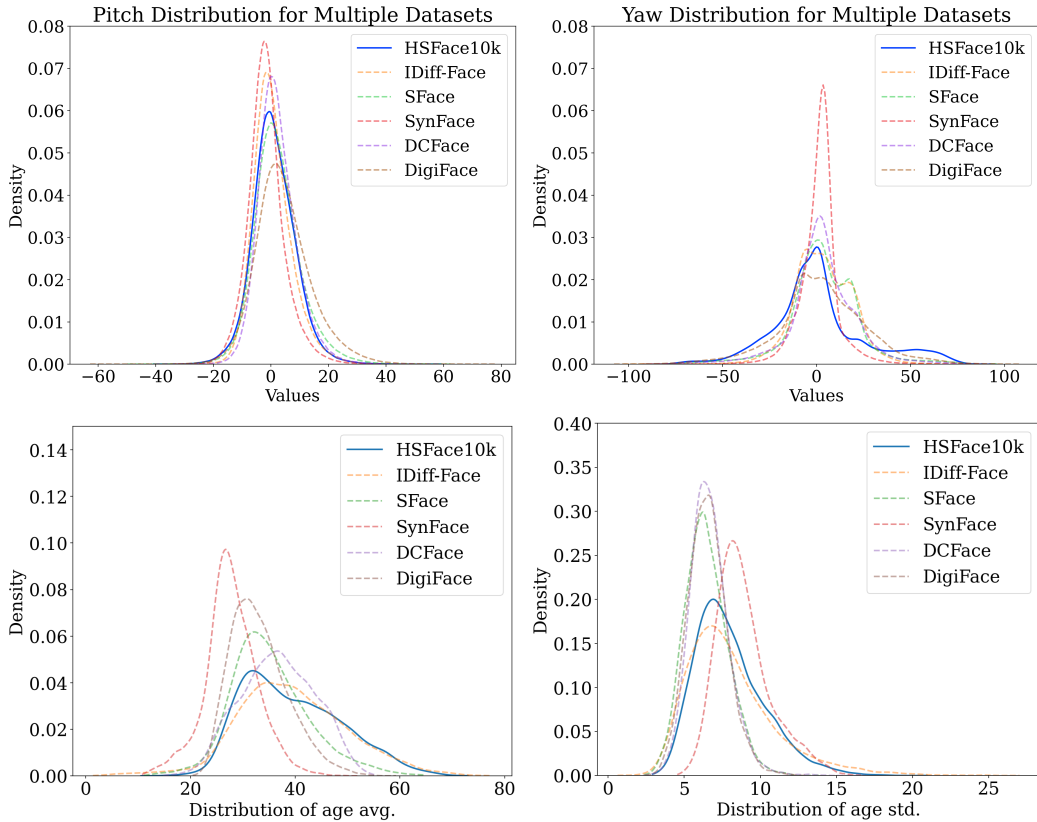


Figure 6: Pose and age variation across five test sets and HSFace10k (ours).

as an inter-class noise. The results show that, except for DCFace and ours, the other datasets have inter-class noise to some extent.

Generally, our proposed dataset has the lowest intra-class noise and inter-class noise. Moreover, Figure 4 shows that the proposed dataset has the lowest overlapped area / Equal Error Rate (EER), showing the best dataset quality on separability between genuine (same people) and impostor (different people) pairs. It promises more reliable identity labels for the FR algorithm to learn better representations.

A.4 THE EFFECT OF AGE AND POSE VARIATION OF DATASETS IN FR ACCURACY

To estimate the distribution of age and pose, we use `img2pose` (Albiero et al., 2021) and an age estimator (Albiero et al., 2020) to obtain the data. Fig. 6 shows the distributions of pose and age of five available synthetic datasets and HSFace10k. Since roll is controlled by face detectors, only pitch and yaw angles are estimated. The results show that all the datasets have large variations on both pose and age, suggesting the accuracy difference is not mainly caused by the attribute variation but by identity consistency. Having large variations but losing the identity consistency results in lower accuracy.

A.5 FEATURE INTERPOLATION AND FEATURE VALUE IMPACT ON GENERATED IMAGES

We analyze the impact of feature values on the generated images in two ways: 1) interpolating six feature vectors between two image features and 2) proportionally changing the values in the feature vector. Figure 7 shows the results of feature interpolation between two images. It indicates that the interpolation in the feature domain can be smoothly presented in the image domain, showcasing Vec2Face’s capability of understanding the vector characteristics in the feature domain. Figure 8 shows the results of proportionally changing the values in the feature. The observations are: 1) As the values in a feature vector increase to a large extent, the image stops changing but the quality

216
217
218
219
220
221
222
223
224
225
226
227
228
229
230
231
232
233
234
235
236
237
238
239
240
241
242
243
244
245
246
247
248
249
250
251
252
253
254
255
256
257
258
259
260
261
262
263
264
265
266
267
268
269

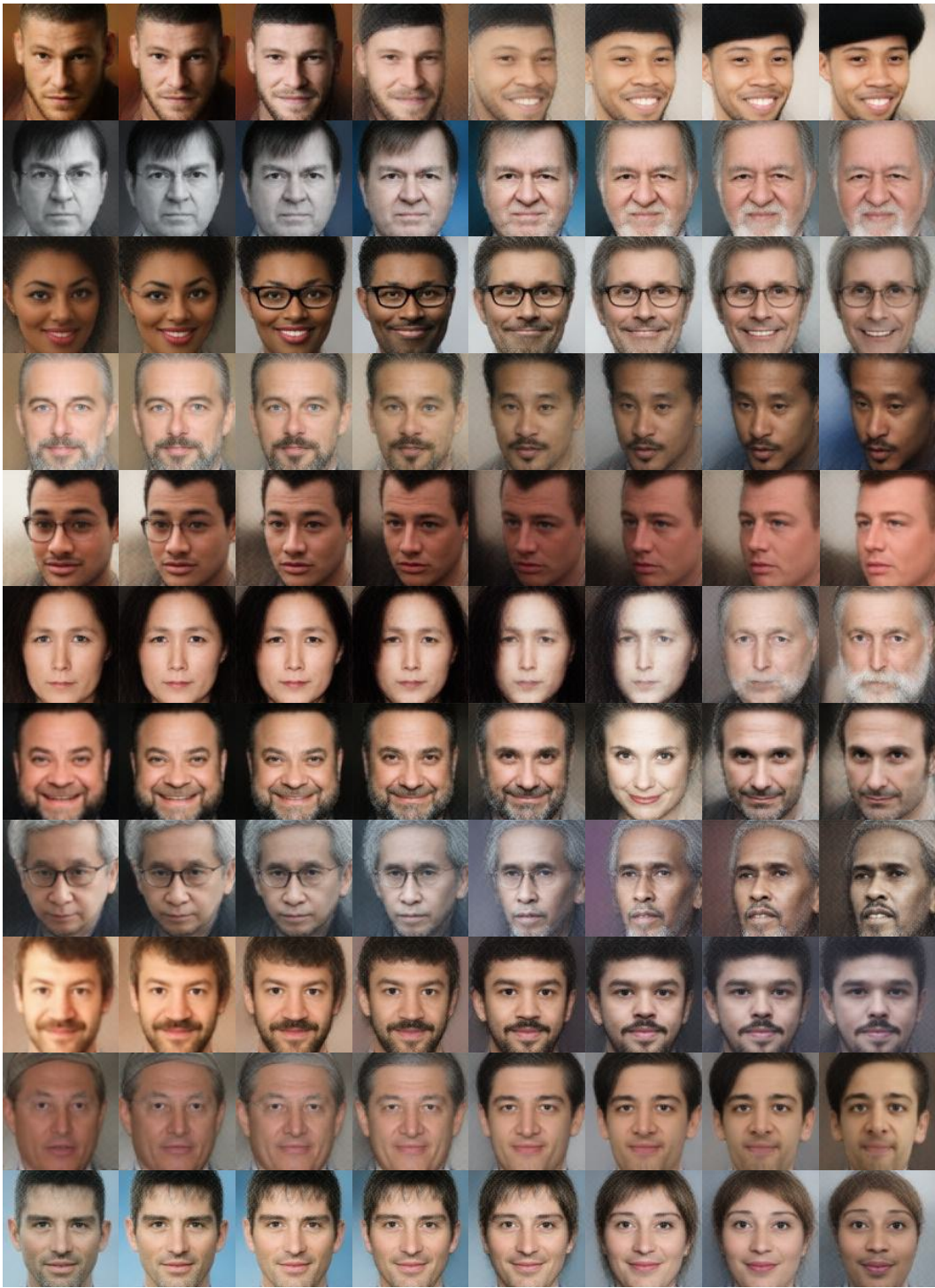


Figure 7: Feature interpolation results. These show that Vec2Face can smoothly convert one image to another by simply changing the feature values.



Figure 8: Impact of feature values analysis. The first row shows images generated with feature values, from left to right, of $\{0, 1, 1.5, 2, 3, 10, 100, 200\}$. The second row shows images generated with feature values of $\{-0.5, -1, -1.5, -2, -3, -10, -100, -200\}$. The last row shows images generated with feature values of $\{1, 0.5, 0.25, 0.125, 0.0625, 0.03125, 0.015625, 0\}$.

decreases, for both negative and positive directions; 2) As the values in a feature vector become close to zero, the face attributes are erased and eventually disappeared.

A.6 IMPACT OF VALUES AT DIMENSIONS

Vec2Face generates an image based on the values in a feature vector, which motivates an intriguing investigation of how values in dimensions impact the output image. We start at changing the value in one dimension. Fig. 13 shows the cases where some obvious patterns occurring. For each of the four identities, the value at index 15 is related to the hair volume, pose angle, age and expression; the value at index 26 have a high correlation with the bangs, facial hair and age, eyeglasses presence, and expression; increasing the value at index 32 changes the age, head pose, hair color, and expression. The observation is that changing values in a single dimension may change the face attribute but it is not consistent for all identities. In fact, changing value at a single dimension does a negligible change on the generated image in most dimensions.

We then change the values in fixed-length (*i.e.*, 8) of dimension chunks and there are some noticeable patterns. Fig. 12 shows the generated images when the values at specific dimensions increases. A general conclusion is that changing values at dimension chunks varies the facial attributes but the patterns are also inconsistent across identities. For instance, dimension $[40:48]$ changes the age for the first identity, no obvious pattern for the second, the expression for the third, and head pose for the fourth; dimension $[56:64]$ changes the hairstyle for the first identity, facial hair for the second, age and eyeglasses for the third, age and facial hair for the fourth; dimension $[96:104]$ changes the gender for the first identity, age and hairstyle for the second, face exposure level for the third, and facial hair for the fourth. Therefore, it is hard to control the attributes by handcrafting the features. AttrOP is much more efficient and effective.

A.7 DISCUSSION OF PRIVACY ISSUE AND FUTURE DATASET USAGE

The privacy issue of using images from real identities is the main concern in face recognition technique development. As a result, governments publish regulations (Voigt & Von dem Bussche, 2017) to restrict the biometric data usage. Before the possible

Datasets	HSFace300K	WebFace4M (50K)	Glint360K
Accuracy	93.52	96.61	97.63

Table 1: FR accuracy comparison of the model trained with the largest proposed data HSFace300K, the 50K identities used for Vec2Face training, and the pretrained FR model used for feature extraction.

fully restrictions on real face data usage, although no achieving as good performance as using datasets of real data (see in Table 1), this work provides several datasets for continuing the development of face recognition techniques without violating the regulations. Moreover, the unique design of Vec2Face can be inspired for generating better synthetic datasets in the future.

324
325
326
327
328
329
330
331
332
333
334
335
336
337
338
339
340
341
342
343
344
345
346
347
348
349
350
351
352
353
354
355
356
357
358
359
360
361
362
363
364
365
366
367
368
369
370
371
372
373
374
375
376
377

A.8 OTHER MATERIAL

The architecture of fMAE is in 10. The FR training configuration is in Table 2. The examples of the effect of stochasticity in fMAE on generated images is in Figure 9.



Figure 9: Examples of the effect of the stochasticity of fMAE. Each vectors is processed 8 times for image generation. The changes on images are negligible.

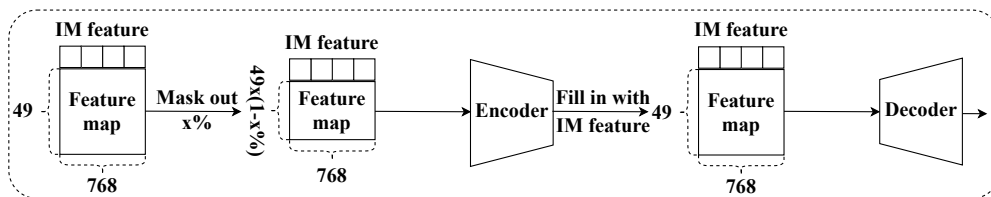


Figure 10: Architecture of the proposed feature masked autoencoder (fMAE).

Face Recognition Model Training Configurations	
Head	ArcFace
Backbone	SE-IR50
Input Size	112×112
Batch Size	128
Learning Rate	0.1
Weight Decay	5e-4
Momentum	0.9
Epochs	26
Margin	0.5
FP16	True
Sample Rate	1.0
Reduce Learning Rate	[12, 20, 24]
Augmentation	Random aug. and Random erase
Optimizer	SGD
Workers	2
GPU	RTX6000

Table 2: Configurations used for synthetic dataset training.

378
379
380
381
382
383
384
385
386
387
388
389
390
391
392
393
394
395
396
397
398
399
400
401
402
403
404
405
406
407
408
409
410
411
412
413
414
415
416
417
418
419
420
421
422
423
424
425
426
427
428
429
430
431

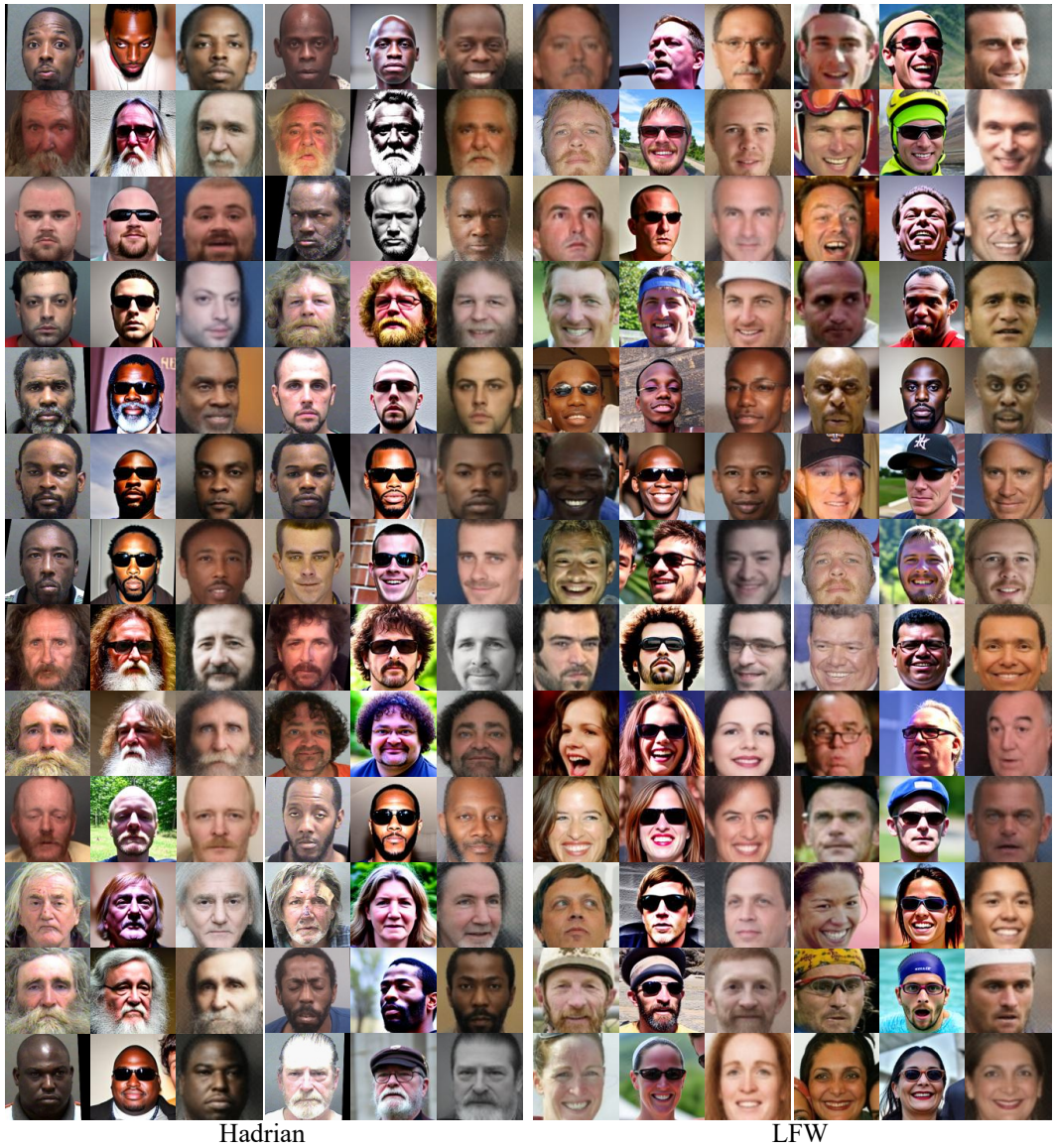


Figure 11: Examples of reconstructed Hadrian and LFW images by Arc2Face and Vec2Face. The images in each three-image group, from left to right, are the original, from Arc2Face, and from Vec2Face.

432
433
434
435
436
437
438
439
440
441
442
443
444
445
446
447
448
449
450
451
452
453
454
455
456
457
458
459
460
461
462
463
464
465
466
467
468
469
470
471
472
473
474
475
476
477
478
479
480
481
482
483
484
485

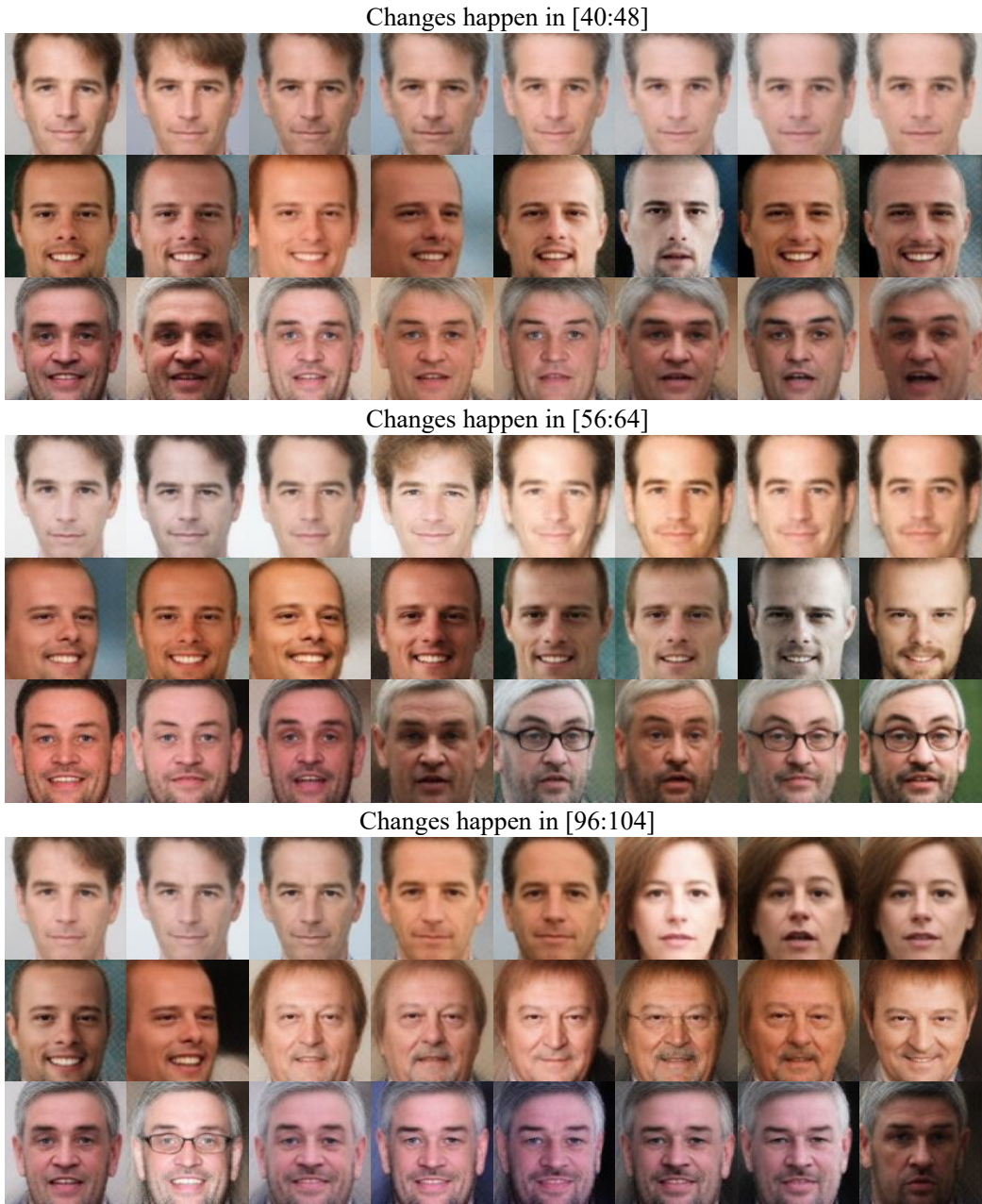
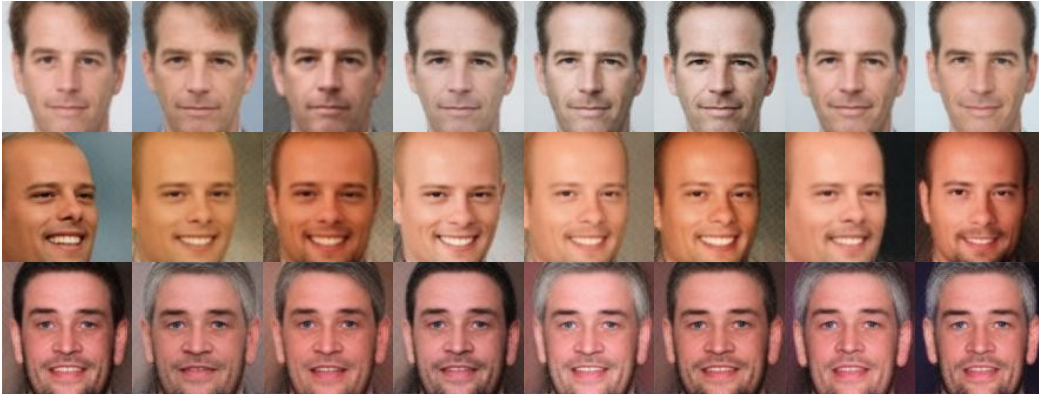


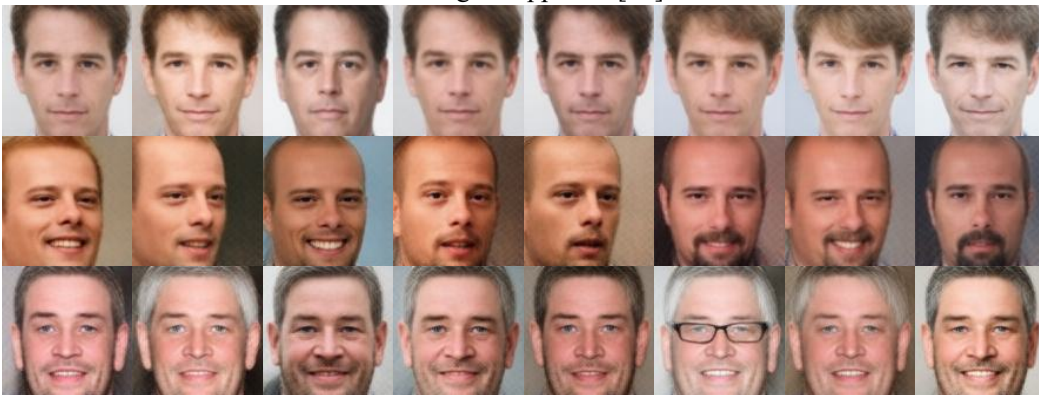
Figure 12: Examples of changing values in a single dimension. From left to right, the value gradually increases in the target dimensions. The raw images are in low quality, so we use AttrOP to increase the image quality.

486
487
488
489
490
491
492
493
494
495
496
497
498
499
500
501
502
503
504
505
506
507
508
509
510
511
512
513
514
515
516
517
518
519
520
521
522
523
524
525
526
527
528
529
530
531
532
533
534
535
536
537
538
539

Changes happen in [15]



Changes happen in [26]



Changes happen in [32]

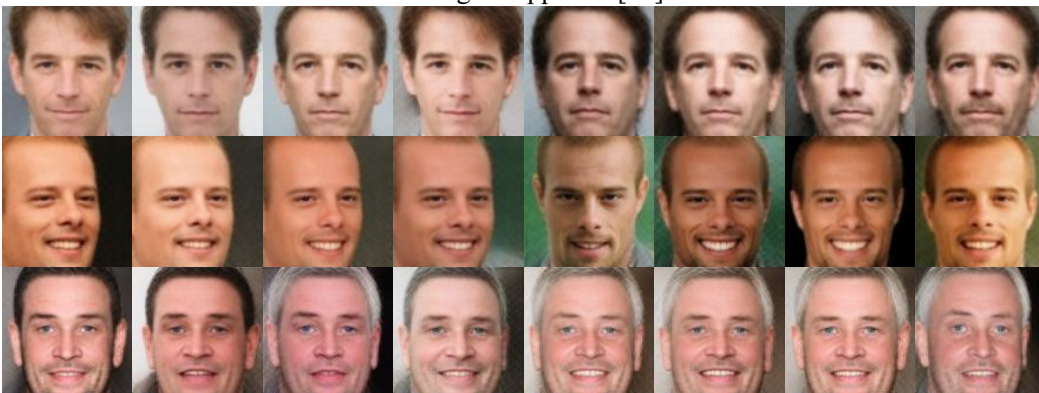


Figure 13: Examples of changing values in a single dimension. From left to right, the value gradually increases in the target dimensions. The raw images are in low quality, so we use AttrOP to increase the image quality.

540
541
542
543
544
545
546
547
548
549
550
551
552
553
554
555
556
557
558
559
560
561
562
563
564
565
566
567
568
569
570
571
572
573
574
575
576
577
578
579
580
581
582
583
584
585
586
587
588
589
590
591
592
593

REFERENCES

- Vítor Albiero, Kai Zhang, and Kevin W Bowyer. How does gender balance in training data affect face recognition accuracy? In *IJCB*, pp. 1–10. IEEE, 2020.
- Vitor Albiero, Xingyu Chen, Xi Yin, Guan Pang, and Tal Hassner. img2pose: Face alignment and detection via 6dof, face pose estimation. In *CVPR*, pp. 7617–7627, 2021.
- Gwangbin Bae, Martin de La Gorce, Tadas Baltrusaitis, Charlie Hewitt, Dong Chen, Julien P. C. Valentin, Roberto Cipolla, and Jingjing Shen. Digiface-1m: 1 million digital face images for face recognition. In *WACV*, pp. 3515–3524, 2023.
- Fadi Boutros, Marco Huber, Patrick Siebke, Tim Rieber, and Naser Damer. Sface: Privacy-friendly and accurate face recognition using synthetic data. In *IJCB*, pp. 1–11. IEEE, 2022.
- Fadi Boutros, Jonas Henry Grebe, Arjan Kuijper, and Naser Damer. Idiff-face: Synthetic-based face recognition through fuzzy identity-conditioned diffusion model. In *ICCV*, pp. 19650–19661, 2023.
- Qiong Cao, Li Shen, Weidi Xie, Omkar M. Parkhi, and Andrew Zisserman. Vggface2: A dataset for recognising faces across pose and age. In *IEEE F&G*, pp. 67–74, 2018.
- Jiankang Deng, Jia Guo, Jing Yang, Niannan Xue, Irene Kotsia, and Stefanos Zafeiriou. Arcface: Additive angular margin loss for deep face recognition. *TPAMI*, 44, 2022.
- Gary B Huang, Marwan Mattar, Tamara Berg, and Eric Learned-Miller. Labeled faces in the wild: A database for studying face recognition in unconstrained environments. In *Workshop on faces in 'Real-Life' Images: detection, alignment, and recognition*, 2008.
- Minchul Kim, Feng Liu, Anil K. Jain, and Xiaoming Liu. Dcfac: Synthetic face generation with dual condition diffusion model. In *CVPR*, pp. 12715–12725. IEEE, 2023.
- Foivos Paraperas Papantoniou, Alexandros Lattas, Stylianos Moschoglou, Jiankang Deng, Bernhard Kainz, and Stefanos Zafeiriou. Arc2face: A foundation model of human faces. *arXiv preprint arXiv:2403.11641*, 2024.
- Haibo Qiu, Baosheng Yu, Dihong Gong, Zhifeng Li, Wei Liu, and Dacheng Tao. Synface: Face recognition with synthetic data. In *ICCV*, pp. 10860–10870, 2021.
- Paul Voigt and Axel Von dem Bussche. The eu general data protection regulation (gdpr). *A Practical Guide, 1st Ed.*, Cham: Springer International Publishing, pp. 10–5555, 2017.
- Haiyu Wu and Kevin W Bowyer. What should be balanced in a balanced face recognition dataset. In *BMVC*, pp. 2, 2023.
- Haiyu Wu, Sicong Tian, Aman Bhatta, Jacob Gutierrez, Grace Bezold, Genesis Argueta, Karl Ricanek Jr., Michael C. King, and Kevin W. Bowyer. What is a goldilocks face verification test? *arXiv preprint arXiv:2405.15965*, 2024.
- Zheng Zhu, Guan Huang, Jiankang Deng, Yun Ye, Junjie Huang, Xinze Chen, Jiagang Zhu, Tian Yang, Dalong Du, Jiwen Lu, and Jie Zhou. Webface260m: A benchmark for million-scale deep face recognition. *TPAMI*, pp. 2627–2644, 2023.